Influence of laser treatment parameters on the mode I strain energy release rate of aluminum double cantilever beam joints

Influence of laser treatment parameters on the mode I strain energy release rate of aluminum double cantilever beam joints

F. Moroni[1], F. Musiari[1], L. Romoli[1], A. Pirondi[1]

[1]Università degli Studi di Parma, Dipartimento di Ingegneria e Architettura. Parco Area delle Scienze 181/A, 43124 Parma, IT.

Corresponding author: fabrizio.moroni@unipr.it (F. Moroni)

Abstract

Surface texturing produced by laser ablation is an efficient and effective technology for treating substrates to improve adhesive bond strength. In the literature, its effect has been extensively studied for different adherends materials, adhesives and laser sources. Laser ablation produces both morphological and chemical modifications of the surfaces, promoting mechanical interlocking and chemical bonding between the adhesive and the substrates. In this work, the effect of pulsed Yb-fiber laser ablation over the quasi-static mode I fracture energy of Double Cantilever Beam (DCB) aluminum bonded joints has been assessed for different combinations of processing parameters, with the aim of optimizing the treatment for industrial purposes. The mechanical tests show that the treatment becomes effective when a laser energy density threshold is overcome. On the other hand, a further increase in the energy density leads to a slight reduction of the joints fracture energy. This is related to the viscosity of the adhesive and to the high roughness produced by high energy treatments, resulting in the presence of air bubbles in the adhesive layer. In order to understand this phenomenon, the treated surfaces are characterized from the morphological point of view using a 3D optical profiler and SEM analysis.

Keywords

A. Fracture Toughness, B. Surface Roughness, B. Surface Treatment, D. interfaces.

1 Introduction

Among the factors able to influence the effectiveness of the adhesive bonding, the state of the surface had been demonstrated to have a key role. In fact, both the morphology and the chemical properties of the surface are crucial to ensure the achievement of an optimal bonding process, having the capability to enhance or weaken the interface between surface and adhesive and therefore promoting the shift of the failure mode from adhesive (the failure initiates and propagates at the interface) to cohesive (the locus of failure is within the adhesive) and viceversa. Nowadays the awareness of the need for proper mechanical, chemical or electro-chemical surface pre-treatments is settled in the common industrial bonding practice. With the aim to join aluminum substrates, some surface treatments appear especially appropriate, like degreasing (usually preparatory to other treatments), etching, pitting, chemical anodizing and grit blasting [1]. While the first ones are useful for the removal of the contaminants on the surface, the last one has the additional benefit consisting of slightly enhancing the surface roughness. In [2] it is possible to find a summary of the features that different surface pretreatments lend to the bond durability of Al alloys and a study dealing with the influence that an increase of the surface roughness through grit blasting has over the durability of Al/epoxy joints. Actually, in general smooth surfaces do not allow the mechanical interlocking effect between the adhesive and the superficial micro-asperities, which is a beneficial phenomenon for increasing the adhesion strength of the bonding joint and for reducing the probability to get an interfacial failure [3]. Moreover, the achievement of a certain level of surface roughness provides an increase of the contact area between substrate and adhesive [4]. With respect to the improvement of the interfacial strength of the bonded joints, an alternative pre-treatment which was successfully employed in many works is the laser ablation. Different benefits are achievable by using this process: laser ablation promotes the cleaning of the surface from natural oxides and dirt layers and the generation of a superficial pattern ensuring the increase of the roughness and of the contact area, as well as an improvement of the wettability and therefore of the surface free energy (SFE). Buchman *et al.* [5] proved that the adhesional shear and tensile strength of Al joints with laser-ablated surfaces increases up to 20% and 120%, respectively, compared with untreated joints. Moreover, a modification of the failure mode, from interfacial to cohesive, occurred. Alfano *et al.* [6] demonstrated that the improvement that the laser treatment brings to the bond toughness of Al/epoxy bonding joints is up to 400% than the one of sand-blasted surfaces. In [7] it was proved that the laser ablation enhances the apparent shear strength of Al/Mg single lap joints bonded with a toughened epoxy up to 30% with respect to joints with grit-blasted surfaces. Rechner *et al.* [8] showed that the tensile shear strength exhibited by laser pre-treated aluminum joints after aging in salt-fog chamber for up to 2000 h was higher than the one belonging to joints which underwent an atmospheric plasma treatment. Once the ideal setting of the laser parameters has been identified, it is possible to tailor the surface texturing in order to optimize the surface roughness with respect to the increase of strength that it lends to the interface. In this regard, it is worth underlining that an analytical relation between the surface roughness and the mechanical strength

in adhesive bonded joints has not been clearly defined yet. Ikegami [9] proposed a theoretical relation between the surface roughness and the bond strength, considering both the effect of the increase of the contact area and the notch effect due to the roughness, but it does not seem to fit well with all kinds of data because of their dispersion. Shahid et al [10] investigated the influence of surface roughness on the cleavage strength of a steel joint, the last one appearing to linearly increase with the roughness level. In [11] some tests were executed in order to identify the trend between the surface roughness and the adhesive strength of carbon and brass bonded joints, resulting in the detection of an optimal value of roughness with respect to the tensile strength, while the peel strength did not exhibit any clear relation with the surface roughness. In [12] and [13] the authors confirmed the well-known fact that an optimal roughness exists within a range, outside of which the adhesive strength drops, resulting in an increasing-decreasing trend of the strength with roughness.

This work concerns the attempt at identifying a trend, which relates the toughness of adhesively bonded joints and the surface status induced by properly setting the laser parameters according to different combinations. In particular, the influence of the surface morphology over the Mode I strain energy release rate of joints with aluminum substrates is assessed. The main objective is to identify critical values of the process parameters able to modify the surface characteristics (in particular, the surface morphology and the distribution of peaks and valleys over the surface were evaluated), in order to maximize the strain energy release rate of the bonding joint.

2 Experimental set-up

2.1 Laser Treatment

In this work a pulsed Nd:YVO4 laser (wave length λ=1064 nm) was used to ablate the surface of the adherends before the bonding process. The laser equipment used for the experiments was intentionally selected among those available for commercial use and provides for a pulse frequency in the range of 1-100 kHz. As a consequence, the cost of this kind of machine is relatively low (if compared with different laser sources/wavelength and higher power) and therefore more suitable for an industrial application. The apparatus was equipped with a z-axis positioning system for focus adjustment and an x-y galvo-mirror scanner. The pulse repetition rate was kept fixed to 20 kHz, and the pulse duration was equal to 140 ns. The diameter of the spot d_s was set to 35 µm through the focusing. The laser ablation was carried out making the beam scan the surface straightly on parallel lines from one end of the processed area to the other. The laser parameters were changed in order to study their effects over the surface morphology and over the mechanical behavior of the joints. The laser parameters studied in this work were the average power of the

beam (*P*) varied in the range 6-18 W, the scan speed (*v*) ranging from 90 to 1000 mm/s, and the hatch distance (*H*) varied between 25 and 100 µm. The effects of the treatments were also evaluated in terms of energy density (*ED*), defined as:

$$ED = \frac{P}{v d_s} \tag{1}$$

This parameter represents the amount of energy irradiated by the laser per unit of surface area. Examples of surfaces resulting from the ablation treatment are shown in Figure 1. Due to the partial overlapping of following pulses (in the vertical direction in the figure below), the treatment produces grooves. The distance between adjacent groves is the hatch distance *H*. The depth of the grooves is roughly related to the parameter *ED:* in a predictable manner, the higher is *ED*, the higher is the energy given to the material and therefore the amount of molten/vaporized material. For higher *ED* values, debris and molten material expelled from the grooves solidifies on their edges, producing crests as shown, for example, in Figure 1 panel c.

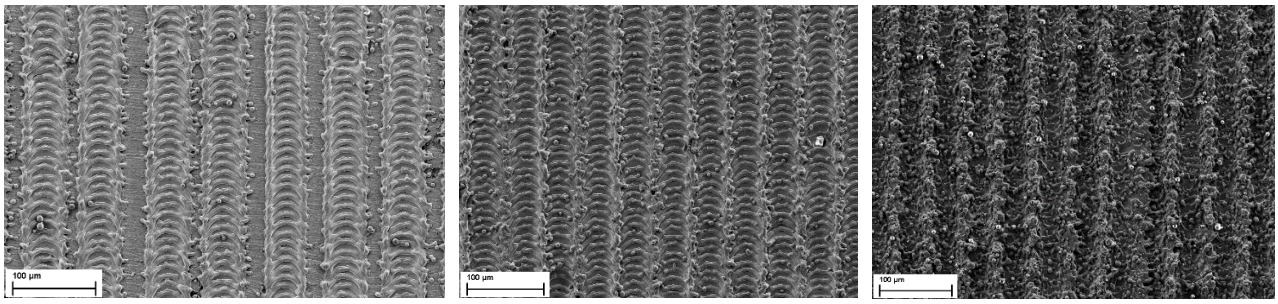

(a) (b) (c)

Figure 1 – Example of SEM observation of laser treated surfaces: a) low ED - wide H, b) low ED - tight H, c) high ED - tight H

2.2 Surface Characterization

For a better understanding of the mechanical behavior of the bonded joint when changing the surface treatment before bonding, the morphology of adherends surfaces was measured using a CCI Taylor-Hobson 3D optical profiler with a resolution of 340 nm on the longitudinal plane and 1 nm on the vertical axis. The morphology maps were used to compute the average surface roughness S_a and the Pearson's first coefficient of skewness (S_{sk}) related to the distribution of the z-coordinate of the profile with respect to the mean plane. The main reason for using the surface parameters (S_a, S_{sk}) instead of the classical profile parameters (such as R_a, R_{sk}) is the better representativeness of the first one in the case of rough, anisotropic surfaces. The average surface roughness [14] is defined as:

$$S_a = \frac{1}{A}\iint |z(x,y)|dxdy \tag{2}$$

In Eq. (2) A is the value of the area over which S_a is calculated, the x-y plane is parallel to the surface while the z-axis is normal to the surface. The surface skewness S_{sk} [14] was calculated using Eq. (3)

$$S_{sk} = \frac{1}{S_q^3 A}\iint z^3(x,y)dxdy \tag{3}$$

Here S_q is the root mean square height of the surface, shown in Eq.(4).

$$S_q = \sqrt{\frac{1}{A}\iint z^2(x,y)dxdy} \tag{4}$$

In a morphology analysis, the surface skewness represents the distribution of the peaks and the valleys with respect to the mean plane of the surface: positive values of S_{sk} mean that the height of the peaks is higher than the depth of the valleys, the opposite is true in the case of negative values of S_{sk}.

Specimens were also studied after the mechanical tests: in order to study the failure locus and the fracture process, a 50X optical microscope was used for observing the morphology of the bonded surfaces after that the breakage occurred.

2.3 *Joint geometry and Materials*

In order to evaluate the influence of the laser parameters on the mode I strain energy release rate, a series of Double Cantilever Beam (DCB) tests was carried out. The joint geometry and dimensions are respectively shown in Figure 2 and Table 1.

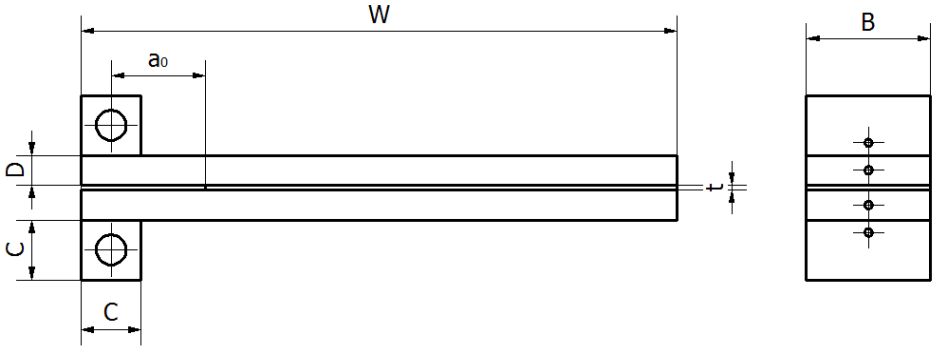

Figure 2 - Joint Geometry

Table 1 - Joint Dimensions

W [mm]	D [mm]	C [mm]	B [mm]	t [mm]	a_0 [mm]
120	6	12	25	0.15	25

The two adherends were manufactured out of a AA 6082-T6 aluminum alloy bar (mechanical properties in Table 2). Small steel blocks were drilled and adhesively bonded over one side of each adherend to transmit the load during the test. Loctite Hysol 9466 (mechanical properties are shown in Table 3), a toughened epoxy two component adhesive, was used to produce the joints.

Table 2 – Substrate mechanical properties [www.matweb.com]

Young Modulus	E_s [GPa]	70
Poisson's Ratio	ν_s	0.33
Tensile Yield Strength	Rp_s [MPa]	260
Tensile Ultimate Strength	Ru_s [MPa]	310

Table 3 – Adhesive mechanical properties [www.henkel.com]

Young Modulus	E_a [MPa]	1718
Poisson's Ratio	ν_a	0.35
Tensile Ultimate Strength	Ru_a [MPa]	32

2.4 Joint Preparation

The adherends were initially washed with soap and water with the intent of cleaning the surfaces from possible residual traces of the machining. This operation was carried out in order to obtain a homogeneous condition for all the specimens and avoid the variability related to the execution of the laser treatment over surfaces covered with different amount of contaminants. Secondly, the surfaces were treated with laser ablation and, within 1 hour, were assembled. The thickness of the adhesive bondline was controlled by using calibrated metal sheets as spacers at both the ends of the specimen. The initial crack was induced by the insertion of a polyester sheet at one extremity of the specimen. The bonded joint underwent a curing cycle at a temperature of 80°C for 1 hour. Simply degreased and grit-blasted specimens were also produced and tested for comparison. The grit blasting was performed using with alumina particles (grade 80). The pressure was set approximately at 0.5 MPa and the nozzle was kept at a distance of about 30 mm from the surface.

2.5 Mechanical Characterization

Mechanical tests were performed according to the international standard ASTM D3433 [15] in a servo-hydraulic testing machine MTS 810 equipped with a 3 kN load cell. The machine was controlled in displacement at a constant cross-head speed and the test was carried out by applying a load-unload law in rate of displacement control (2 mm/min in the loading phase and 4 mm/min in the unloading phase), since the actual crack length during the test was evaluated by the compliance method. For this purpose, an omega clip gage was applied in front of the specimen to measure the Crack Opening Displacement (COD) during the test (Figure 3).

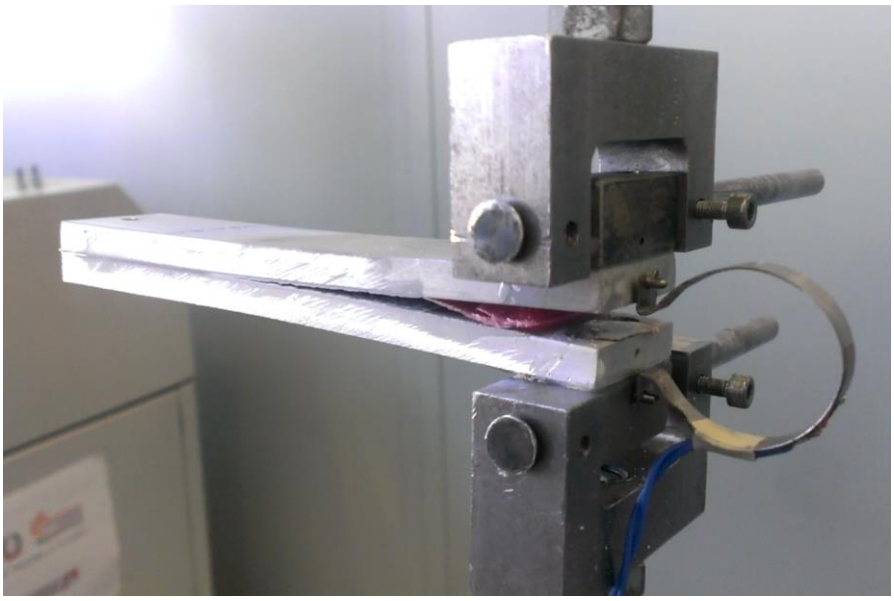

Figure 3 – Execution of the DCB test

Once the crack length was known, the Mode I energy release rate G_I was calculated in correspondence of each peak force using the Krenk model [16]:

$$G_I = \frac{12(P_{MAX}a)^2}{B^2 E_s D^3}\left(1 + \frac{1}{a\lambda_\sigma}\right)^2 \tag{5}$$

where P_{MAX} is the peak force, a is the actual crack length, λ_σ is a correction parameter whose expression is given in eq (2).

$$\lambda_\sigma = \sqrt[4]{\frac{6}{D^3 t}\frac{E_a}{E_s(1-\nu_a^2)}} \tag{6}$$

Figure 4 shows an example of the Load vs. COD plot for a DCB test (panel a), and the result in terms of Strain Energy Release rate (G_I) as a function of the crack length a (panel b). The adhesive predominantly showed a ductile behavior and the R-curve was almost flat for each tested specimen. The critical strain energy release rate G_{IC} was therefore computed for each joint as the average of the plateau values. A total of 21 tests were carried out on laser treated specimens, each one having different value of P, v or H.

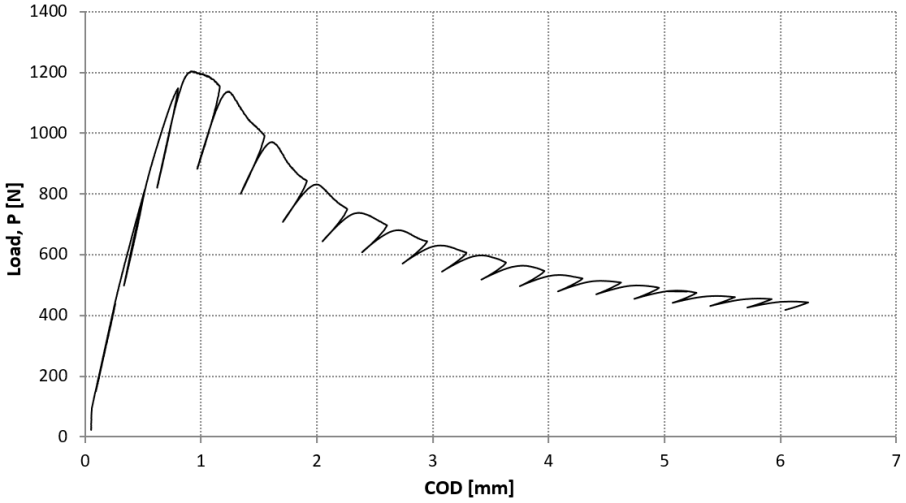

(a)

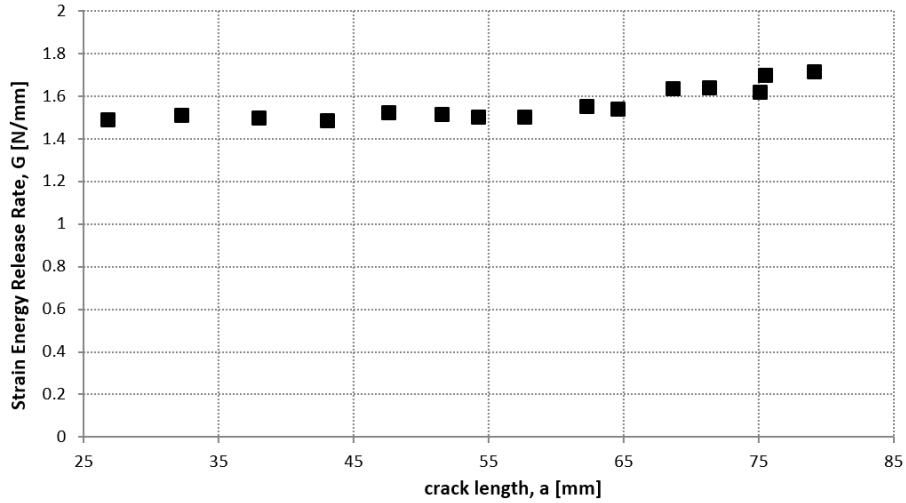

(b)

Figure 4 – Example of Load vs. COD (a) resulting and R curve (b) in a DCB test

3 Results and discussion

3.1 Surface Characterization

In carrying out the characterization of the surfaces when changing the laser process parameters, a first noticeable correlation was the one between the surface roughness S_a and the energy density *ED*, as shown in Figure 5. As already noticed in [17], S_a seemed steadily increasing as *ED* grew up, at least until *ED* reached a threshold value, approximately equal to 4.0 J/mm^2. When *ED* overcame this value, the surface roughness S_a slightly decreased.

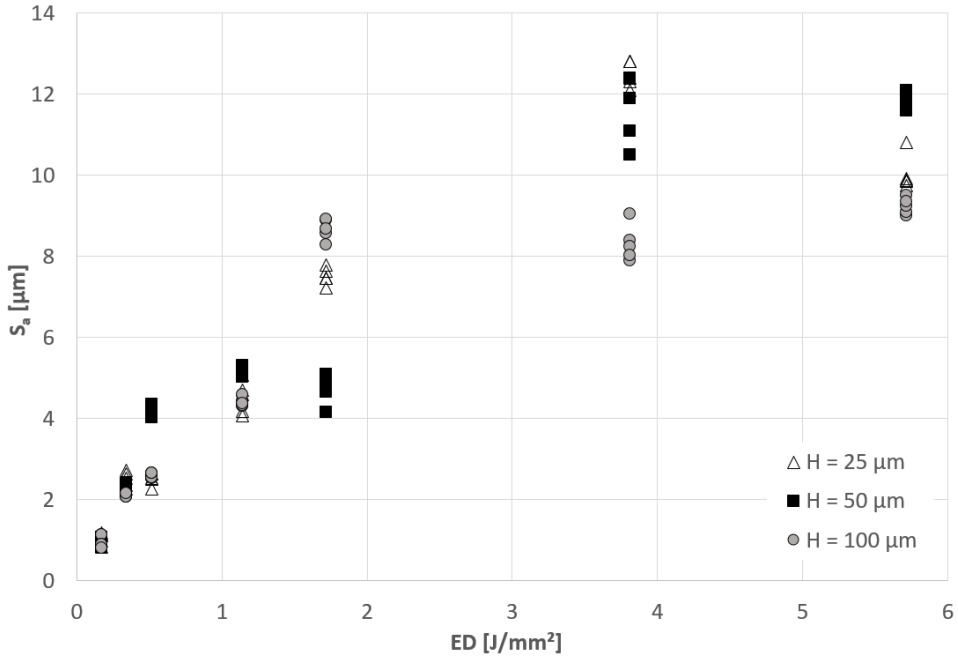

Figure 5 – Measured valued of surface average roughness (S_a) vs Energy density (ED) for different hatch distances (H)

This phenomenon was probably due to the softening of the bulk material caused by the higher levels of *ED* and subsequently to the fact that peaks and valleys of the surface patterns induced by the laser ablation were closer to each other. With respect to the dependence of the hatch distance *H* with the surface roughness, *H* = 100 µm set exhibited lower values than the other two, with the exception of the values in correspondence of *ED* = 1.7 J/mm^2 at which the trend seemed flip.

The trend of S_{sk} in function of *ED* is showed in Figure 6. In correspondence of very low values of *ED* (0.17 J/mm^2), S_{sk} assumed negative values because the energy was not high enough to produce a significant ablation, the only modification with respect to the original surface being the generation of slightly deep valleys over the treated surface.

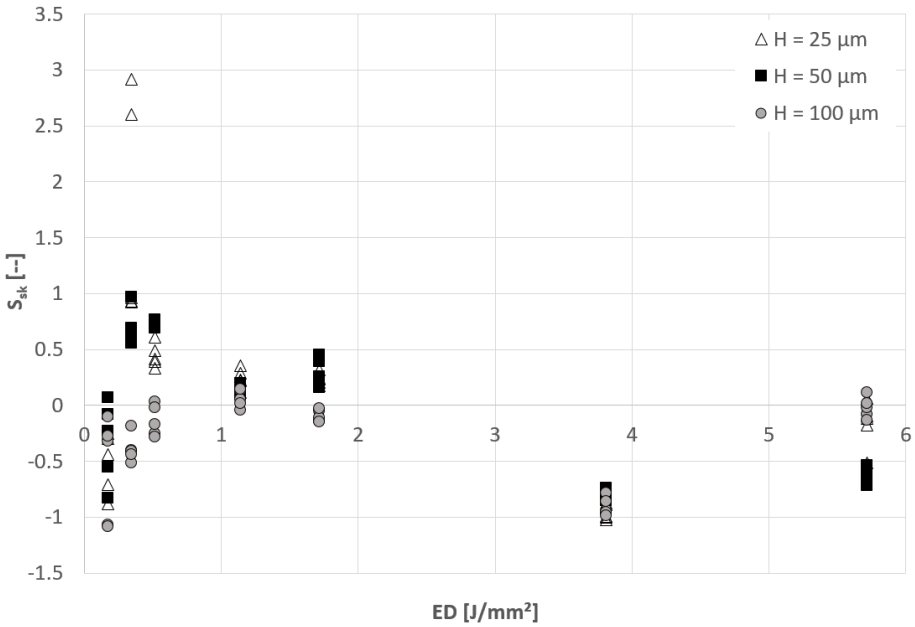

Figure 6 – Measured valued of surface skewness (S_{sk}) vs Energy density (ED) for different hatch distances (H)

As *ED* rose up to 0.34 J/mm^2, the interaction between ablated material belonging to adjacent grooves increased but the behavior of S_{sk} was diversified: for high values of the hatch distance (H = 100 µm) the surface skewness S_{sk} remained negative, but as H decreased S_{sk} became increasingly positive, until it reached values ranging from 2.6 and 3 for the case of H = 25 µm. The more a superposition between adjacent grooves was present, the more the surface morphology was characterized by the presence of peaks due to the stacking of ejected material. A further increase of *ED* resulted in a lowering of S_{sk} until a minimum (when ED = 3.8 J/mm^2) and finally in a slight increase to values close to zero. This is due to the fact that, as the available energy for the process grew up, the effectiveness of the laser ablation increased and so did the depth of the valleys produced by the treatment. It is worth noting that when H = 100 µm the values of S_{sk} remained approximately always negative throughout the entire explored energy density field.

In order to appreciate the differences in surface morphology, some 400x400 µm tridimensional maps extracted from the profilometer reconstruction and SEM observation of the treated surfaces are shown in Figure 7.

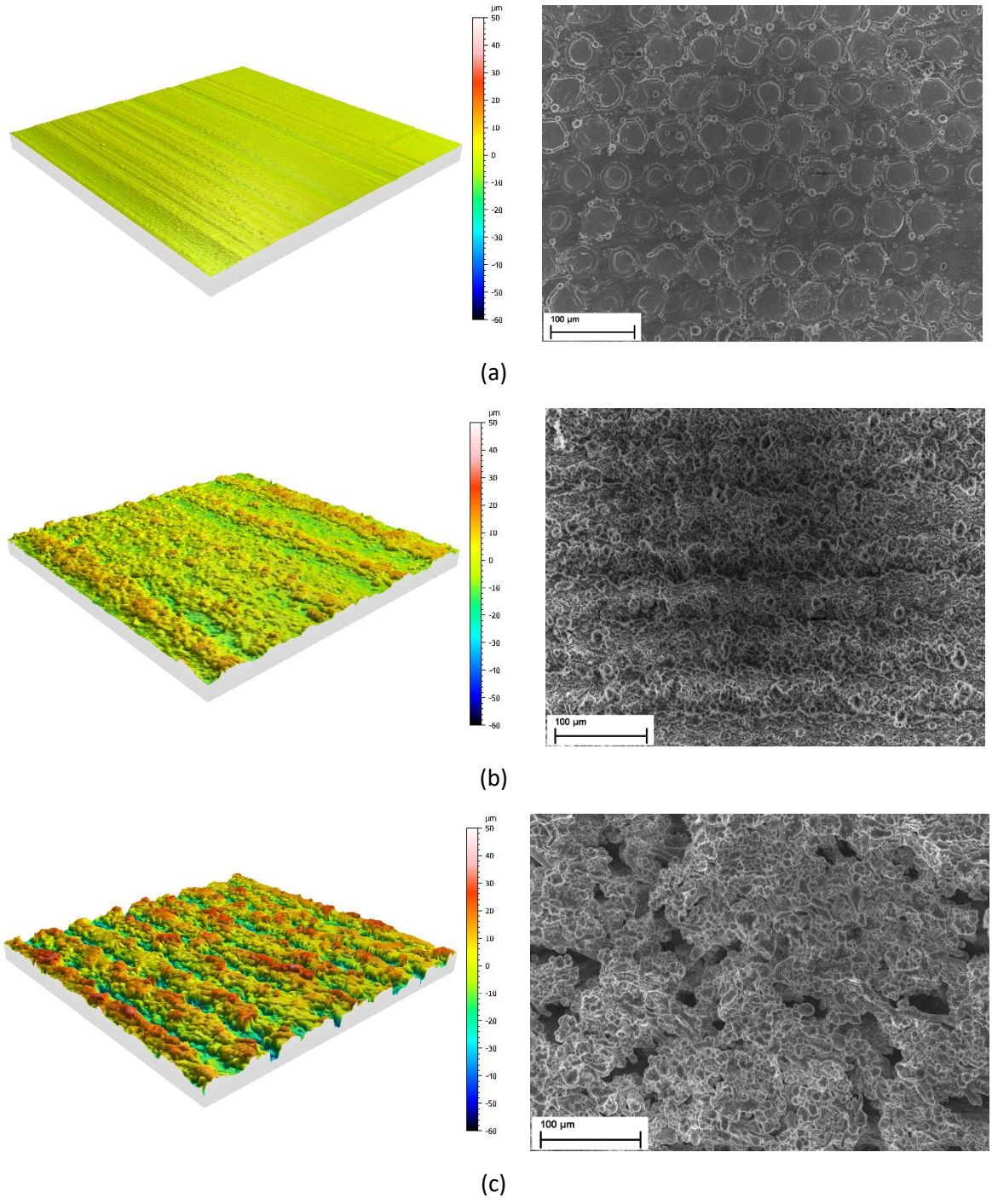

Figure 7 – Comparison between profilometer morphology (left) and SEM observation (right) of surfaces produced with H = 50 µm and: a) P = 6 W and v = 1000mm/s (ED = 0.17 J/mm²), b) P = 18 W and v = 300 mm/s (ED = 1.7 J/mm²), c) P = 18 W and v = 90 mm/s (ED = 5.7 J/mm²).

The images refer to surfaces whose laser treatment was characterized by the same hatch distance *H* = 50 µm. The surface of the panel "a" (*ED* = 0.17 J/mm^2) was approximately flat: here *ED* was just above the energy threshold of the surface ablation, and only some small cavities were produced on the surface. In correspondence of *ED* = 1.7 J/mm^2 (panel "b") the surface morphology was significantly modified by the ablation. This surface was rougher than the previous one and the height of the peaks seemed greater than

the depth of the valleys, resulting in positive values of S_{sk}. Finally, when *ED* = 5.7 J/mm^2 the surface was still rougher than the aforementioned and it was characterized by deep grooves. As a consequence, the distance between the mean plane and the bottom of the surface was higher with respect to the distance from mean plane and the top, which is why the value of S_{sk} appeared to be negative.

Figure 8 proposes a second kind of comparison between surface configurations with the same value of *ED* (0.34 J/mm^2) and progressively increased value of *H* (25 – 50 – 100 µm).

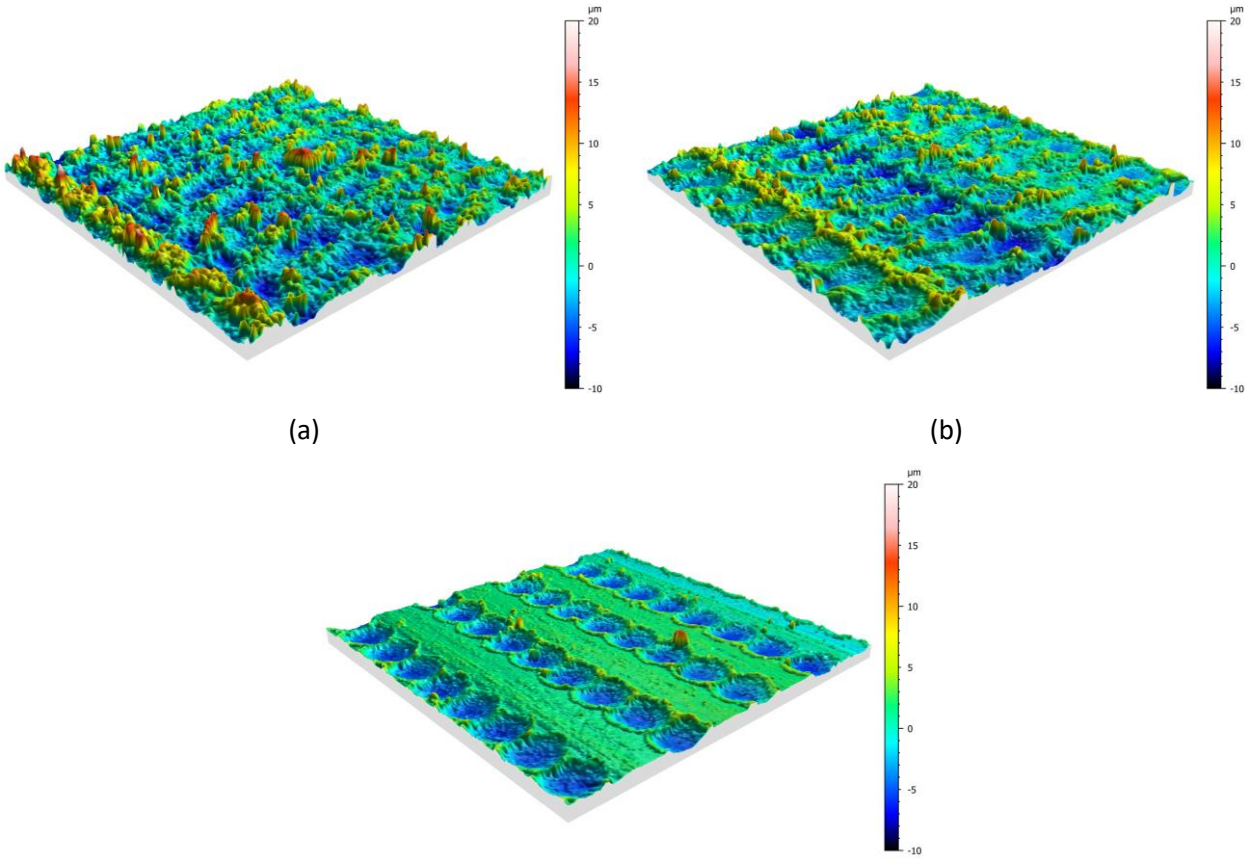

Figure 8 – Comparison among surfaces morphology produced with ED = 0.34 J/mm² (P = 12 W and v = 1000mm/s) and: a) H = 25 µm, b) H = 50 µm, c) H = 100 µm.

The average surface roughness (S_a) of the three specimens was almost the same (Figure 5). On the other hand, they presented significantly different morphologies and extremely different values of skewness coefficients. The first surface showed a sort of a low level mean plane with some crests produced by the interaction between adjacent grooves. The second surface was instead characterized by a balanced sequence of peaks and valleys. Finally, the third surface showed the untreated surface with some craters on it. For these three morphology maps, the skewness factor progressively decreases moving from the first to the latter, as it can be noticed in Figure 6.

For comparison purposes, also grit blasted and simply degreased surfaces were measured. Figure 9 shows their morphology maps, while their surface parameters are indicated in Table 4. The resulting roughness

values are close to the typical values for a cold drawn bar [18] and for a grit blasted surfaces [19]. The untreated surfaces are macroscopically smooth and their roughness is close to those of the laser treated specimens with the lower ED values. Moreover, their skewness coefficient is close to zero indicating a symmetric distribution of the profile height.

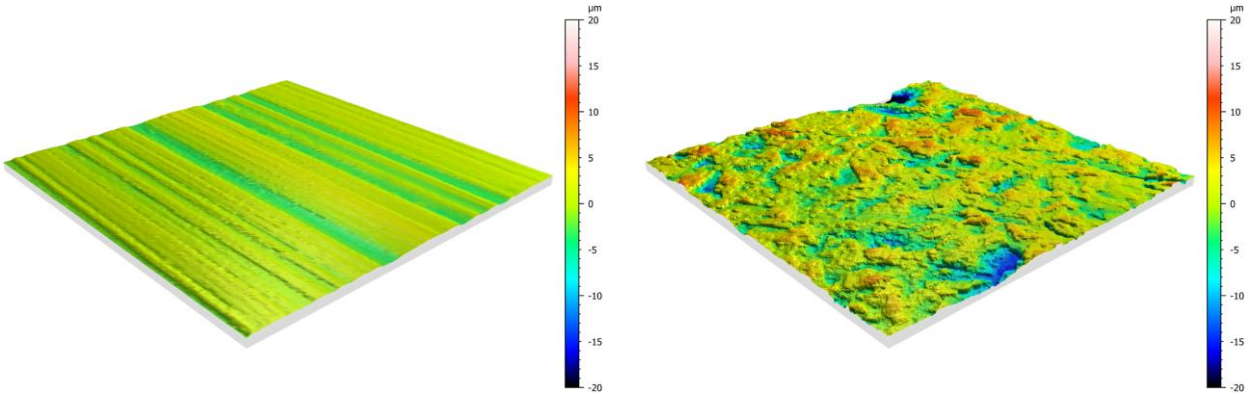

(a) (b)

Figure 9 – Comparison between surfaces morphology of untreated and grit blasted surfaces.

Table 4 – Surface Parameters for Degreased and Grit Blasted surfaces

Parameter	**Degreased**	**Grit Blasted**
S_a [µm]	1.20	3.16
S_{sk} [--]	-0.182	-1.07

The grit blasted surfaces are obviously rougher then the untreated and show a skewness coefficient lower than zero, indicating a surface predominantly characterized by valley.

3.2 Mechanical Characterization

The DCB joints were produced and tested. The results in terms of the mechanical strength were studied and discussed as a function of surface and treatment parameters.

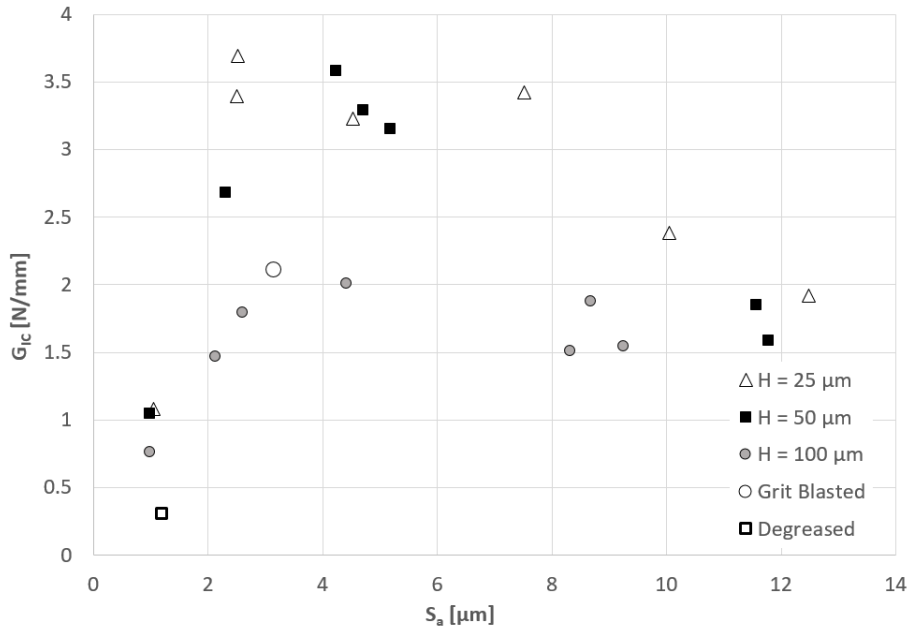

Figure 10 – Mode I strain energy release rate (G_I) vs average surface roughness (S_a) for laser treated and grit blasted DCB joints.

In Figure 10, the mode I strain energy release rate G_{IC} obtained with the DCB tests is plotted as a function of the surface roughness S_a. The S_a values plotted in this graph are the mean values obtained with the same laser parameters. First of all, it can be seen that the laser treatment can yield joints up to 65% stronger than grit blasted joints. Moreover, it is possible to notice how the values of G_I are strongly dependent on the value of the hatch distance *H*. Nevertheless, the trend that G_I exhibited as S_a grew was approximately the same: G_I increased until reaching a maximum at a certain level of S_a (different for each value of *H*), then G_I decreased as S_a further rose up.

An analogue trend was found when plotting the mode I strain energy release rate as a function of the energy density *ED* (Figure 11). It is worth underlining that, when the hatch distance *H* was closer or lower than the diameter of the spot d_s, the values of the mode I strain energy release rate G_{IC} became fairly independent from *H*. Instead, when the distance between adjacent grooves significantly exceeded the diameter of the spot, lower values of fracture toughness are obtained, independent of *ED*.

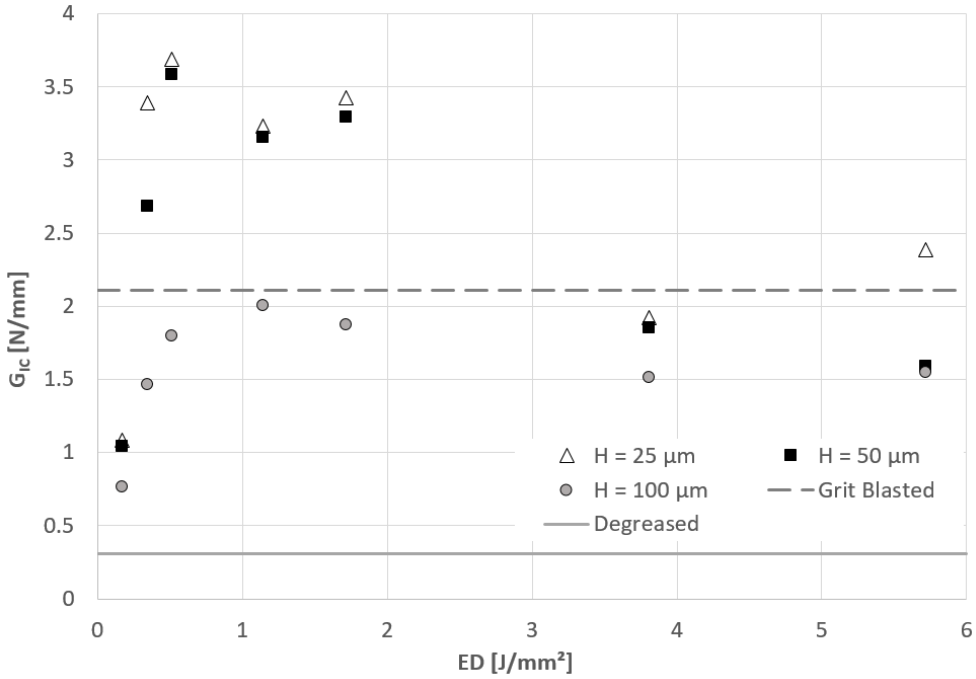

Figure 11 – Mode I strain energy release rate (G_I) vs Energy Density (ED) for laser treated DCB joints. The value resulting from Grit blasted joints and degreased joints are also indicated as reference.

3.3 Study of the fractured surfaces

The trends of G_I shown in Figure 10 and Figure 11 were justified observing the post-failure appearance of the bonded surface with a 50X optical microscope. When the energy density was very low (0.17 J/mm²), the treatment did not succeed to effectively modifying the surface morphology, resulting in a complete adhesive failure of the interface, Figure 12.

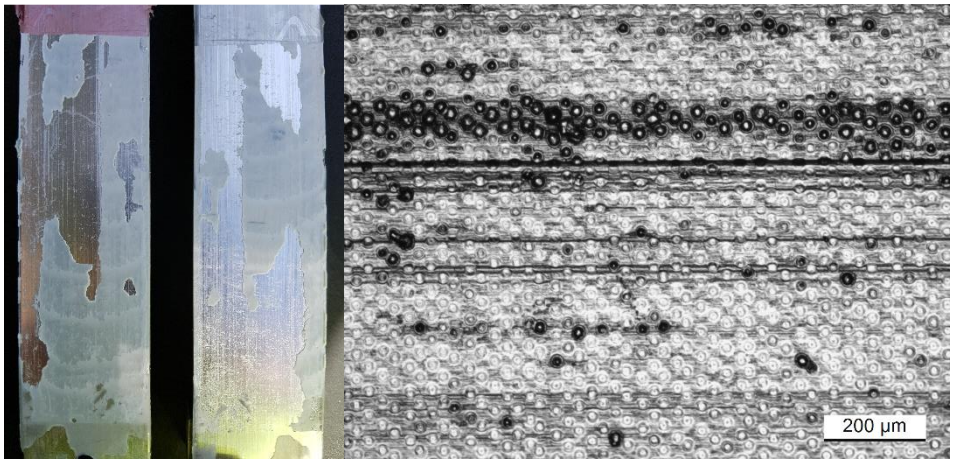

Figure 12 – Fracture surface in the case of P = 6 W, v = 1000 mm/s and H = 25 µm (ED = 0.17 J/mm²)

As *ED* increased (in the range between 0.34 and 1.7 J/mm²), for joints produced with *H* equal to 25 or 50 µm, the fracture appeared completely cohesive as shown in Figure 13. This means that the treatment succeeded

in the modification of the surface morphology, promoting the interlocking between adhesive and aluminum substrate.

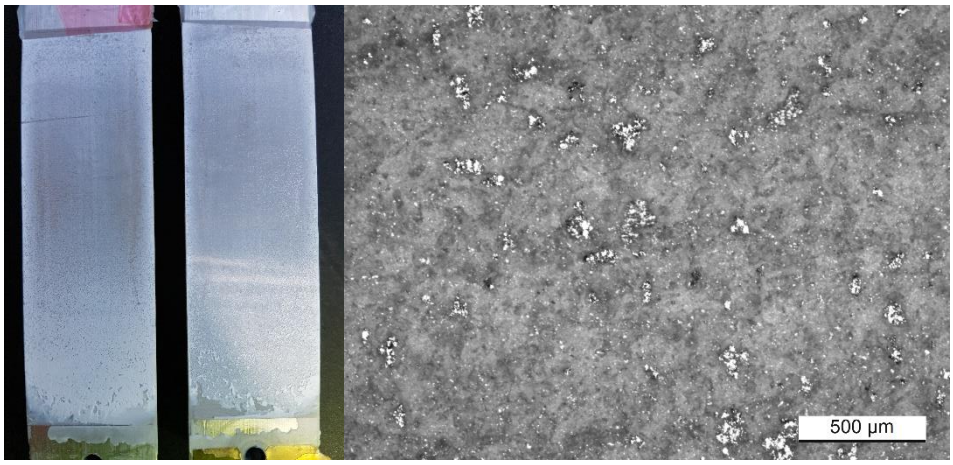

Figure 13 – Fracture surface in the case of P = 18 W, v = 1000 mm/s and H = 50 µm (ED = 0.51 J/mm²)

A further *ED* increase produced a significant modification of the surface fracture. For example, Figure 14 shows the failure in the case of *ED* = 1.1 J/mm². Although the fracture was still completely cohesive, some air bubbles were identified (black spots in the right picture). The treatment succeeded in promoting adhesion, but at the same time, within the grooves produced by the treatment, small amount of air remained entrapped.

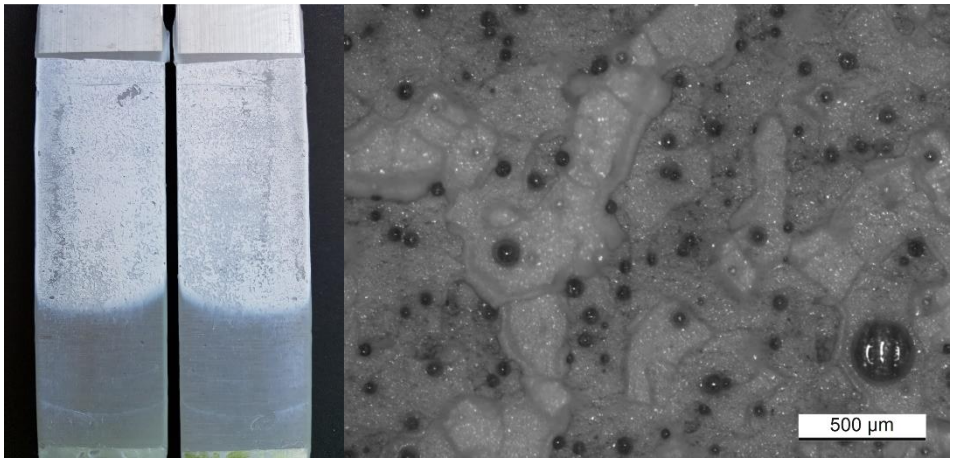

Figure 14 – Fracture surface in the case of P = 12 W, v = 300 mm/s and H = 50 µm (ED = 1.1 J/mm²)

The higher the *ED*, the deeper the grooves, and therefore the higher was the amount of air trapped. This can be noticed in Figure 15, resulting from a joint treated with *ED* = 3.8 J/mm², where a huge amount of air bubbles (black dots) can be identified. Obviously, the presence of voids in the adhesive layer weakened the adhesive strength, inducing the failure to propagate at lower values of energy. This phenomenon can

therefore explain the decrease of the measured strain energy release rate noticed beyond 2 J/mm² in Figure 11.

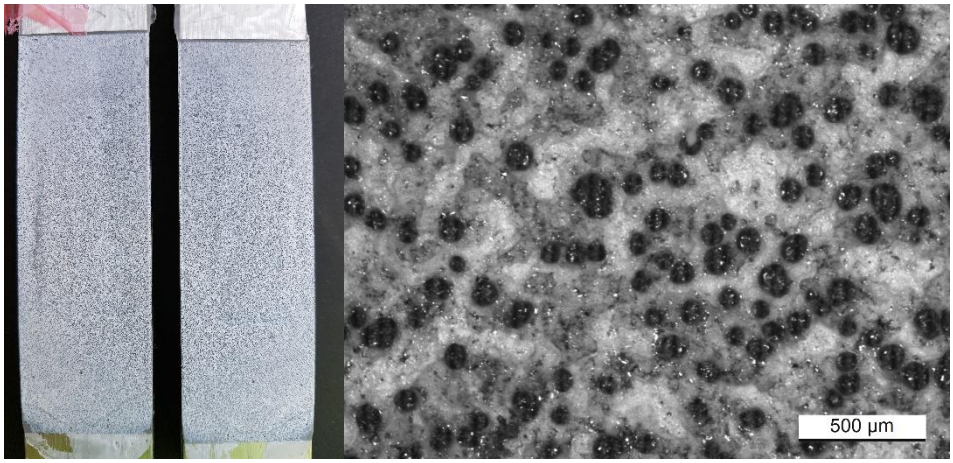

Figure 15 – Fracture surface in the case of P = 12 W, v = 90 mm/s and H = 50 µm (ED = 3.8 J/mm²)

When dealing with laser treatment carried out with hatch distance, *H*, significantly higher than the spot diameter (d_s = 35 µm), a partial adhesive/cohesive failure appeared, as shown in Figure 16. The rate of surface affected by the laser treatment was smaller than previous cases, which resulted in an increase of the amount of surface undergoing adhesive failure and therefore in a substantial reduction of the strength of the bonded joint.

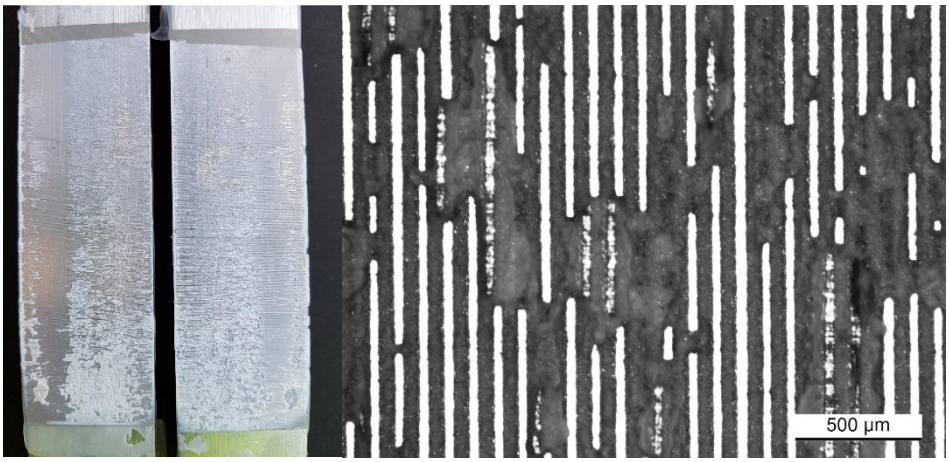

Figure 16 – Fracture surface in the case of P = 18 W, v = 300 mm/s and H = 100 µm (ED = 1.7 J/mm²)

Two different phenomena appeared therefore to be relevant for the failure process of treated joints:

a) The laser surface treatment should be able to modify the surface morphology to increase the interlocking effect between adhesive and adherend and therefore ensure a cohesive failure

b) The surface modification should not create too narrow grooves to avoid air entrapment during the adhesive deposition, and therefore weaken the adhesion.

The average surface roughness S_a could be a good indicator of the interlocking effect as demonstrated in literature ([10], [20][17]) but it is not able to catch the differences of the surfaces in terms of peaks and valley, governing the air entrapment phenomenon. Figure 17 shows the mode I strain energy release rate G_{IS} vs surface skewness S_{sk} plot. The aim is to relate the strain energy release rate with surface morphological parameters, especially considering the peak/valley distribution.

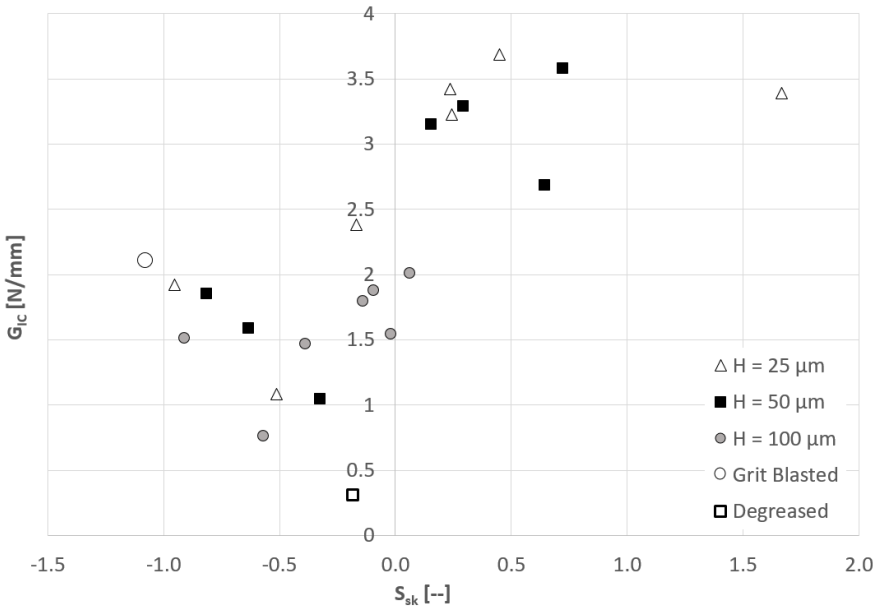

Figure 17 – Mode I strain energy release rate (G_I) vs surface skewness (S_{sk}) for laser treated and grit blasted DCB joints.

Despite the considerable dispersion of data, it was possible to identify an increasing trend of G_I with S_{sk}, which appeared meaningful since the prevalence of peaks in the surface morphology enhanced the possibility to have a mechanical interlocking effect between substrate and adhesive, which resulted in an increase of the fracture toughening of the bonding joint. Moreover, the curve summarizes some results already noticed in Figure 10 and Figure 11 related to the *H* = 100 µm set. For that value of hatch distance, the surface skewness was negative at every value of *ED* (except the maximum one, 5.7 J/mm^2, at which the surface skewness was slightly above zero), so there was a prevalence of valleys with respect to the mean plane of the surface and the mechanical interlocking effect was low. Hence, the adhesive failure mode prevailed over the cohesive and the mode I strain energy release rate required to damage propagation was below the values measured when a certain level of overlap between the grooves was present.

Figure 17 provided also the opportunity to notice that in general, the lower the values of S_{sk}, the higher was the amount of entrapped air within the valleys because of their depth. Therefore, the surfaces with the lowest values of surface skewness were the ones revealing the highest presence of bubbles when they

underwent microscopic examination. This is the reason why the mode I strain energy release rate G_I decreased when ED reached the highest values of the explored range, in correspondence of which the surface skewness S_{sk} was very low.

4 Conclusions

In this work the influence of the laser treatment parameters on the strain energy release rate of DCB aluminium bonded joints was investigated. The results of the experimental tests indicated that the treatment succeeded in modifying the surface in promoting the interlocking between adhesive and adherends. For this purpose, the energy density plays a key role: in order to maximise the joint strength, the energy density should be above a threshold value (0.5 J/mm²), to ensure a significant morphological modification. At the same time, it should not exceed 2 J/mm² in order to avoid the generation of deep grooves, scarcely filled by adhesive. Also the hatch distance assumes an important role: in order to maximise the strength its value should be close to the value of the spot diameter. Wider distances reduce the ratio between the treated surface with respect to the total bonding surface, therefore producing a reduction of the joint strength. Shorter hatch distances do not lead to any further increase of the joint strength; they only produce a disadvantageous increase of the treatment time. The strain energy release rate was also studied as a function of the surface skewness. It appears that the latter is a good indicator of the joint strength since it is able to catch the asymmetry in the distribution of peaks and valley, and therefore the amount of air trapped during the adhesive deposition.

5 Acknowledgments

This research was partially supported by the Italian Ministry for University and Research (MIUR), grant SIR RBSI146ZYJ.

6 References

[1] Bruzzone AAG, Costa HL, Lonardo PM, Lucca DA. Advances in engineered surfaces for functional performance, CIRP Ann - Manuf Techn. 2008; 57 (2): 750-769. *doi: 10.1016/j.cirp.2008.09.003.*

[2] Critchlow GW, Brewis DM. Review of surface pretreatments for aluminium alloys. Int J Adhes Adhes. 1996; 16(4), 255-275. *doi: 10.1016/S0143-7496(96)00014-0.*

[3] Kim WS, Yun IH, Jung HT. Evaluation of mechanical interlock effect on adhesion strength of polymer-metal interfaces using micro-patterned surface topography. Int J Adhes Adhes. 2010; 30 (6): 408-417. *doi: 10.1016/j.ijadhadh.2010.05.004.*

[4] Harris AF, Beevers A. The effects of grit-blasting on surface properties for adhesion. Int J Adhes Adhes. 1999; 19 (6): 445-452. *doi: 10.1016/S0143-7496(98)00061-X.*

[5] Buchman A, Rotel M, Dodiuk-Kenig H. Nd:YAG laser surface treatment of various materials to enhance adhesion. In: Mittal KL, Bahners T editors. Laser surface modification and adhesion, Wiley Publishing; 2015, p. 3-54. *doi: 10.1002/9781118831670.ch1.*

[6] Alfano M, Lubineau G, Furgiuele F, Paulino GH. On the enhancement of bond toughness for Al/epoxy T-peel joints with laser treated surfaces. Int J Fracture. 2011; 171: 139-150. *doi: 10.1007/s10704-011-9636-4.*

[7] Alfano M, Ambrogio G, Crea F, Filice L, Furgiuele F. Influence of laser surface modification on bonding strength of Al/Mg adhesive joints, J. Adhesion Sci. Technol. 2011; 25: 1261-1276. *doi: 10.1163/016942410X533381.*

[8] Rechner R, Jansen I, Beyer E. Influence on the strength and aging resistance of aluminium joints by laser pre-treatment and surface modification. Int J Adhes Adhes. 2010; 30 (7): 595-601. *doi: 10.1016/j.ijadhadh.2010.05.009.*

[9] Ikegami K. Recent trend of adhesivley bonding technology (1996) J. Jpn. Screw Threads Fasteners. 1996; 27(7), 207

[10] Shahid M, Hashim SA. Effect of surface roughness on the strength of cleavage joints. Int J Adhes Adhes. 2002; 22: 235–244. *doi: 10.1016/S0143-7496(01)00059-8.*

[11] Uehara K, Sakurai M. Bonding strength of adhesives and surface roughness of joined parts, J Mater Process Tech. 2002; 127: 178-181. *doi: 10.1016/S0924-0136(02)00122-X.*

[12] Sekercioglu T, Rende H, Gulzos A, Meran C. The effects of surface roughness on the strength of adhesively bonded cylindrical components, J Mater Process Tech. 2003; 142: 82-86. *doi: 10.1016/S0924-0136(03)00463-1.*

[13] Budhe S, Ghumatkar A, Birajdar N, Banea MD. Effect of surface roughness using different adherend materials on the adhesive bond strength, Appl Adhes Sci, 2015; 3-20, *doi: 10.1186/s40563-015-0050-4.*

[14] ISO 25178-2:2012. Geometrical product specifications (GPS) — Surface texture: Areal. Part 2: Terms, definitions and surface texture parameters. 2012.

[15] ASTM D3433 – 99. Standard Test Method for Fracture Strength in Cleavage of Adhesives in Bonded Metal Joints. 1999.

[16] Krenk S. Energy Release Rate of Symmetric adhesive joints, Eng Fract Mech. 1992; 43: 549-559. *doi: 10.1016/0013-7944(92)90198-N.*

[17] Romoli L, Moroni F, Khan MMA. A study on the influence of surface laser texturing on the adhesive strength of bonded joints in aluminum alloys. CIRP Ann - Manuf Techn. 2017; 66: 237-240. *doi: 10.1016/j.cirp.2017.04.123.*

[18] Smith EH, Mechanical Engineer's Reference Book. Butterworth-Heinemann, 1998.

[19] Slătineanu L, Potârniche L, Coteaţă M, Grigoraş I, Gherman L, Negoescu F, Surface roughness at aluminium parts sand blasting. Proceedings in Manufacturing Systems, 2011; 6 (2): 69-74.

[20] Boutar Y, Naïmi S, Mezlini S, Sik Ali MB. Effect of surface treatment on the shear strength of aluminium adhesive single-lap joints for automotive applications. Int J Adhes Adhes. 2016; 67: 38–43, *doi: 10.1016/j.ijadhadh.2015.12.023.*